RECENT BEAUTY PHYSICS RESULTS FROM ARGUS

DAVID BRITTON
Physics Department, McGill University,
Montreal, Province of Quebec, H3A 2T8, Canada

(Representing the ARGUS Collaboration*)

ABSTRACT

Recent results on B meson decays are reported from the ARGUS experiment, which operates at the DORIS II e^+e^- storage ring at DESY. Evidence is presented for the first observation of an exclusive b-u decay in the channel $B^- \to \rho^0 \ell^- \nu$. A preliminary branching ratio of $(1.13 \pm 0.36 \pm 0.26) \times 10^{-3}$ is reported, from which the ratio $|V_{ub}|/|V_{cb}|$ is calculated and found to be in agreement with inclusive measurements.

The inclusive and exclusive production of D_S^+ mesons from B decays are examined. The eight branching ratios of the form $B \to D_s^{(*)} D^{(*)}$ are measured, most of them for the first time. The weak decay constant f_{Ds} is calculated within the framework of heavy quark effective theory ($f_{Ds} = 267 \pm 28$ MeV), and according to the BSW model ($f_{Ds} = 288 \pm 29$ MeV).

A new measurement of the the BR($B^- \to D^{*0} \ell^- \overline{\nu}$) is reported, featuring the full reconstruction of the D^{*0} mesons. This permits an estimate of $|V_{cb}| = 0.045 \pm 0.009$, again using heavy quark effective theory.

1. Observation[a] of the decay $B^- \to \rho^0 \ell^- \nu$

1.1. Introduction

In 1990 the first evidence for direct coupling between the first and third quark generation was reported[1] as an excess of leptons with momentum above 2.31 GeV/c in the inclusive lepton spectrum from B meson decays. This value represents the kinematic limit for leptons accompanying b-quark to c-quark (b-c) transitions, but if the b-quark also decays directly to the lighter u-quark (b-u) the lepton momentum may extend up to 2.64 GeV/c. This evidence was subsequently strengthened by the complete reconstruction of two b-u events.[2]

In the Standard Model this direct coupling between the first and third generations is represented by a non-zero value of the V_{ub} element in the Cabbibo-Kobayashi-Maskawa (CKM) matrix. However, extracting a value for V_{ub} from the inclusive lepton spectrum signal is difficult because the leptons are only observed in a small part of the momentum spectrum (2.31 to 2.64 GeV/c) and the signal must then be extrapolated over the full range according to one of several quite different models. This problem may be somewhat circumvented if an exclusive b-u decay mode is identified, since a much greater range of lepton momenta may be used.

At ARGUS, the first evidence for an exclusive b-u decay has been observed in the channel* $B^- \to \rho^0 \ell^- \nu$. The momentum distribution of the leptons, as calculated according to three different models,[3-5] is shown in Fig.1. The variation between models arises in part from the absolute normalisation, that is, from the calculation of the hadronic matrix element $< \rho | j_\mu | B >$, but particularly from the q^2 dependence of the form factors. This is reflected in the the relative amount of longitudinal and transverse polarisation as a function of momentum, as shown in Fig.2 from the model of WBS.[3] Three conclusions may be drawn from these figures:

- As stated above, the measurement of an exclusive b-u decay mode such as $B^- \to \rho^0 \ell^- \nu$ can reduce the model dependency in extracting information on V_{ub} because the leptons are measured over a greater momentum region (1.5-2.6 GeV/c in this analysis, compared with 2.3-2.6 GeV/c in the inclusive work).
- A comparison of the results from the inclusive and exclusive measurements may help to distinguish between the various theoretical predictions.
- Ultimately, the measurement of the ρ polarisation would allow the model ambiguity to be resolved from the exclusive measurement alone.

Unfortunately, at this stage the amount of data is insufficient to allow more than the first report of evidence for an exclusive b-u decay, and some very preliminary estimates of V_{ub}.

*References to a specific charged state also imply the charge conjugate state.

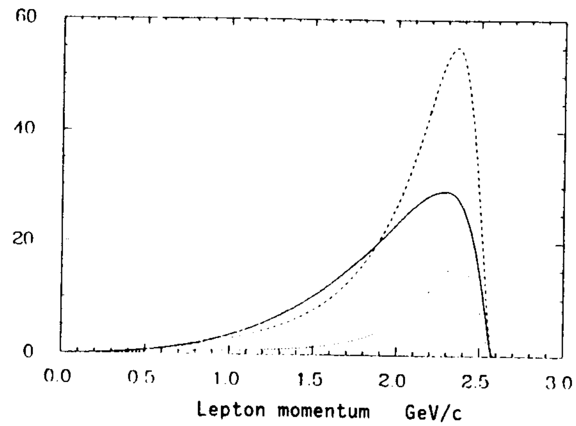

Figure 1: The momentum distribution of leptons in $B^- \to \rho^0 \ell^- \nu$ decay according to the models of KS[4] (dashed curve), WBS[3] (solid curve), and ISGW[5] (dotted curve).

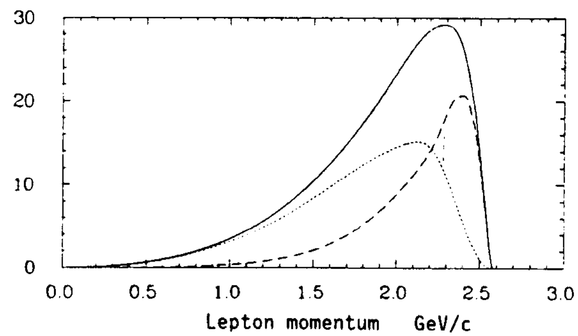

Figure 2: The momentum spectra of leptons accompanying transverse (dashed) and longitudinal (dotted) polarised ρ mesons in the decay $B^- \to \rho^0 \ell^- \nu$ according to the model of WBS.[3]

1.2 Data analysis

The decay $B^- \rightarrow \rho^0\ell^-\nu$ was isolated by making full use of the various kinematic constraints available, and identified as a ρ mass peak in the $\pi\pi$ mass spectrum of Υ_{4s} events containing at least one lepton. The data sample consisted of 234 pb^{-1} of integrated luminosity taken on the Υ_{4s} resonance. The ARGUS detector, its trigger and particle identification capabilities are described in detail elsewhere.[9] To make full use of the kinematic characteristics, the data were divided into a single and di-lepton sample. The cuts enumerated first are applicable to the single lepton sample.

1. To ensure that the kinematics of the event was consistent with a missing neutrino, the magnitude of the missing momentum in the event was required to be greater than 1 GeV/c. The missing momentum is defined as the vector sum of the momenta of all the measured particles.

2. If only the ρ candidate, the lepton, and the neutrino, come from the decay of one B meson, and all the other particles in the event from the decay of the other B meson (the second' B), then there should be no correlation between the thrust axis of the $\rho\ell$ system and the thrust axis of the rest of the event. If this hypothesis is not true then a correlation between the two halves of the event is introduced and the distribution of the angle between the two thrust axes peaks at $|\cos(\theta_{th})| = 1$. Therefore, $|\cos(\theta_{th})| < 0.7$ was required.

3. The momentum of the lepton was required to be between 1.5 and 2.6 GeV/c, the momentum of the pion pair forming the ρ candidate was required to be greater than 0.8 GeV/c, and the product of the lepton and pion pair momenta was required to be greater than 2.0 GeV^2/c^2. These cuts, optimised from Monte Carlo studies, exploit the slightly harder lepton momentum spectrum for b-u transitions than for b-c transitions, as discussed above; and the fact that the momentum distribution of pion pairs forming the combinatorial background is softer than that of pion pairs from ρ decay.

4. The mass recoiling against the $\rho\ell$ system was required to be consistent with a zero mass neutrino. All the necessary kinematic quantities are known except the angle between the B meson momentum and that of the $\rho\ell$ system. The cut was applied requiring the cosine of the calculated angle to satisfy $|\cos(\theta_{B,\ell\pi\pi})| < 1 + \sigma$, where σ represents the measurement uncertainties.

5. The mass recoiling against the second' B meson should be zero for the single lepton sample, or positive for the di-lepton sample or if some particles were missed from the reconstructed event. The finite detector resolution leads to an optimised cut requiring the missing mass squared $M^2 > -0.5$ GeV^2/c^4.

6. The average magnitude of the transverse momentum of B mesons produced at ARGUS is 250 ± 200 MeV/c and the average magnitude in the beam direction is 0 ± 450 MeV/c. These numbers are compared with the momentum of the second' B meson and a χ^2 calculated. Events are rejected when $\chi^2 > 4$.

7. The energy of the B meson calculated from the sum of the energies of the $\ell\pi\pi$ system and the neutrino was normalised to the beam energy and required to lie between 0.96 and 1.08. The slight asymmetry in this cut reflects the fact that for b-c transitions the neutrino energy tends to be somewhat smaller than in b-u transitions.

The total acceptance of all the above cuts applied to the single lepton sample is 14% for $B \rightarrow \rho\ell\nu$ and 0.12% for the background from other Υ_{4s} decays. For the analysis of the di-lepton sample, cuts 3, 4, and 5 are used along with two additional constraints:

8. Events from the underlying continuum tend to be more jet-like than true Υ_{4s} decays; therefore, the cosine of the angle between the two leptons is required to be greater than -0.8.

9. Since the assumption is now that the second B meson also decays semileptonically, the mass recoiling against the lepton is limited to a maximum of 2.1 GeV/c^2, to be consistent with a charmed meson.

The total acceptance for the di-lepton sample is 37% for $B^- \rightarrow \rho^0\ell^-\nu$ and 1% for the background from other Υ_{4s} decays.

The $\pi\pi$ mass spectrum resulting from the combined single and di-lepton analysis of Υ_{4s} data is shown by the unshaded histogram in Fig.3; the shaded histogram shows the prediction of a Monte Carlo containing only b-c decays; and the hatched histogram is the result of applying the analysis to continuum data. A clear enhancement is observed around the ρ mass of 770 MeV/c^2 (recall that the ρ meson has a natural width of about 150 MeV/c^2). The sharp peak at about 1.8 GeV/c^2 is a reflection from the decay $D^0 \rightarrow K^-\pi^+$ where the kaon is mis-identified as a pion. Various consistency checks were performed:

- The enhancement at the ρ mass is present in both the single and di-lepton samples.
- The signal is visible if the data is divided into electron and muon samples.
- The signal disappears if the B meson mass sidebands are selected.
- The signal disappears if the wrong charge $\ell^\pm\pi^\mp\pi^\mp$ combinations are chosen.
- The analogous decay $B \rightarrow D^0\ell\nu$ is analysed in a similar manner with the D^0 meson decaying to $K^-\pi^+$ (c.f. $B^- \rightarrow \rho^0\ell^-\nu$ and $\rho \rightarrow \pi^+\pi^-$). A signal of 37 ± 6 events is observed in agreement with a Monte Carlo prediction of 34.8 events.

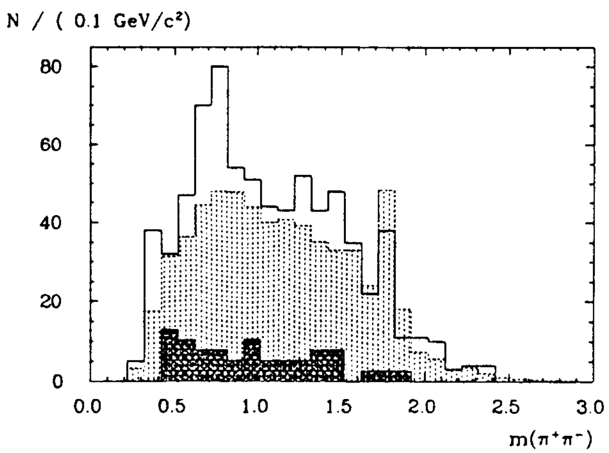

Figure 3: The unshaded histogram shows the $\pi\pi$ mass spectrum from combined single and di-lepton samples. The shaded histogram shows the prediction of a Monte Carlo generating only b-c decays, and the hatched histogram shows continuum data.

1.3. *Results*

In addition to the residual b-c and continuum components, one further background must be considered: the contribution from b-u processes other than $B^- \to \rho^0 \ell^- \nu$. This, obviously, must rely on the predictions of a specific model but the variation between models is accounted for in the final systematic uncertainty. Using the model of Isgur *et al.*,[5] b-u decays of the form $B \to X_u \ell \nu$ were generated where X_u had masses up to 1.7 GeV/c^2. Figure 4 shows the resulting $\pi\pi$ mass distribution for all b-u processes (unshaded histogram) and for all b-u processes except $B^- \to \rho^0 \ell^- \nu$ (shaded histogram).

The points with error bars in Fig.5 show the Υ_{4s} data after subtraction of the continuum contribution. To extract a signal for $B^- \to \rho^0 \ell^- \nu$ this distribution was fitted with the Monte Carlo b-c and b-u components with free amplitudes. The ratio of b-u background to $B^- \to \rho^0 \ell^- \nu$ signal was fixed from Fig.4. The result of the fit is shown by the unshaded histogram; the shaded histogram shows the b-c component. To estimate the systematic error, the amount of b-u background relative to $B^- \to \rho^0 \ell^- \nu$ was varied by a factor of two, the ratio of D^* to D meson production in the b-c Monte Carlo was changed by 30%, and various other models were used to generate the shape of the b-u distribution.

The kinematic region defined by cut 3 above contains between 57% and 65% of the $B^- \to \rho^0 \ell^- \nu$ decays, depending on the model chosen. Using that of Bauer *et al.*,[3] which predicts a value of 61%, a preliminary branching ratio is obtained:

$$BR(B^- \to \rho \ell^- \nu) = (1.13 \pm 0.36 \pm 0.26) \times 10^{-3} \qquad (Preliminary), \qquad (1)$$

where the first error is statistical and the second is systematic. From this result the ratio of $|V_{ub}|/|V_{cb}|$ may be calculated and compared to the results from the inclusive measurements.[2] The results according to the various models are tabulated in Table 1 ($|V_{cb}| = 0.05$ is used).

Table 1: Calculation of $|V_{ub}|/|V_{cb}|$ according to various models.

Model	Exclusive Analysis	Inclusive Analysis[2]
KS[4]	0.15 ± 0.03	0.11 ± 0.01
BSW[3]	0.17 ± 0.03	0.13 ± 0.02
ISGW[5]	0.30 ± 0.06	0.20 ± 0.02
KP[6]	0.15 ± 0.03	0.15 ± 0.02
KSM[7]	0.11 ± 0.02	
ACM[8]		0.11 ± 0.01

1.4. *Conclusions*

Evidence for the exclusive decay $B \to \rho \ell \nu$ has been observed at ARGUS. The results are still preliminary but the values extracted for $|V_{ub}|$ are consistent

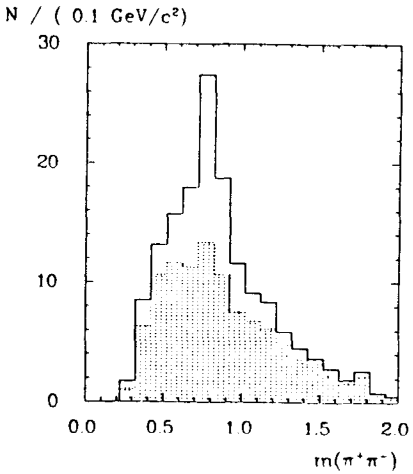

Figure 4: The unshaded histogram shows the $\pi\pi$ mass spectrum from all b-u decays of the type $B \rightarrow X_u \ell \nu$ ($X_u < 1.7$ GeV/c^2) calculated from the model of ISGW.[5] The shaded histogram shows same distribution without the contribution from $B^- \rightarrow \rho^0 \ell^- \nu$.

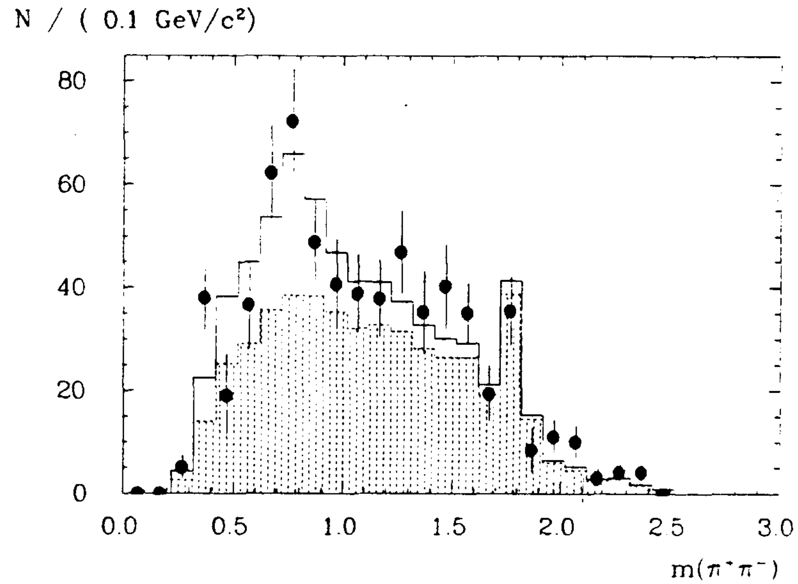

Figure 5: The data points with error bars show the $\pi\pi$ mass spectrum from combined single and di-lepton samples after subtraction of the scaled continuum contribution. The unshaded histogram is the fit result (see text), and the shaded histogram is the b-c component obtained in the fit.

with those from the inclusive measurements. At present the errors are too large to provide precise information but the future comparison of inclusive and exclusive measurements may help distinguish between various theoretical models of weak decays. Ultimately, the measurement of the ρ polarisation would provide additional information since the various models predict quite different ratios of longitudinally and transversely polarised ρ's as a function of momentum.

2. Production[b] of D_S mesons, and the measurement of f_{D_S}

2.1. *Introduction*

The weak decays of B mesons are a premium tool for investigation of the CKM matrix elements, and for testing the various models of heavy flavor decay. At present, only about 12% of the exclusive hadronic decay modes have been observed, mostly in the channels $B \to D^{(*)}n\pi$ and $B \to J/\psi K^{(*)}$. Reported here are measurements of inclusive D_S production, and of a special class of exclusive two-body B decays to double-charm final states. These decays take place via the process $b \to cW$ where the W couples to $c\bar{s}$ quark pair as shown in Fig. 6. Eight exclusive modes of the form $B \to D_S^{(*)}D^{(*)}$ are measured, almost doubling the tally of exclusively reconstructed hadronic decay modes.

The weak decay constant of a meson, such as f_{D_S}, is a measure of the probability that the two constituent quarks annihilate. It therefore determines the purely leptonic decay rate of the meson where the two quarks annihilate forming a W boson, and is a basic dynamical property of a bound $q\bar{q}$ system related to its size. In addition, knowledge of heavy meson decay constants is essential in extracting information on the elements of the CKM quark mixing matrix from weak decay processes.

In the theoretical description of two-body hadronic decay modes a factorisation approach is normally assumed. This idea works well for semileptonic decays which are described by the product of a leptonic and hadronic current. It is assumed that this idea may be extended to the hadronic modes, with the decay amplitude given by the product:

$$< D|j_\nu|B > \cdot < 0|j_\mu|D_S > \quad . \tag{2}$$

The second term represents the production of the D_S meson from the vacuum by the coupling of the W boson to the $c\bar{s}$ quark pair (see Fig. 6). This is just the time-reversal of purely leptonic D_S decay and, therefore, may be expressed in terms of the weak decay constant f_{D_S} :

$$< 0|j_\mu|D_S >= q^\mu f_{D_S} \ , \tag{3}$$

where q^μ is the four-momentum of the D_S. The decays of the form $B \to D_S^{(*)}D^{(*)}$ are particularly well suited to determine f_{D_S} since these final states cannot be produced by the internal W emission diagram shown in Fig. 7.

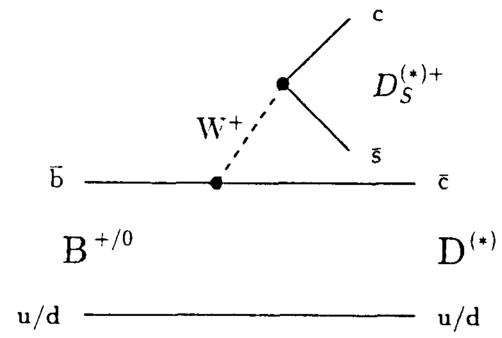

Figure 6: Spectator diagram for double-charm B meson decays.

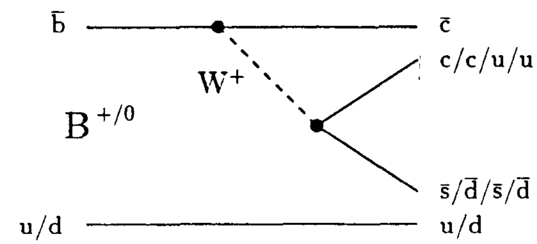

Figure 7: Internal W emission diagram for hadronic B meson decays.

The data used in this analysis consisted off 246 pb^{-1} of Υ_{4s} data and a 109 pb^{-1} continuum sample.

2.2. Inclusive D_S production

The inclusive production of D_S mesons was studied using the decay mode $D_S \rightarrow \phi\pi$. Those K^+K^- candidates within ± 12 MeV/c^2 of the nominal ϕ mass were accepted as ϕ candidates and combined with all the charged pions in the event. Two topological cuts are applied to suppress the combinatorial background (described in more detail in Ref.[10]): $\cos\theta_\phi < 0.8$ is required, where θ_ϕ is angle between the ϕ direction and the D_S boost direction in the D_S rest frame; and $|\cos\theta_K| > 0.5$, where θ_K is the helicity angle of one kaon in the ϕ rest frame, with respect to the pion.

The D_S signal observed in the $\phi\pi$ invariant mass distribution, shown in Fig. 8, was fitted in bins of scaled momentum:

$$x_p = p_{\phi\pi}/p_{max}, \quad \text{where} \quad p_{max} = \sqrt{(E^2_{beam} - m^2_{\phi\pi})}\,. \tag{4}$$

The momentum of D_S mesons from B decays is limited to $x_p < 0.5$, whilst continuum production gives rise to a distribution peaked above $x_p = 0.5$ and extending to 1.0. The measured x_p distributions, corrected for efficiency, are shown in Fig. 9. The continuum sample, and the portion of the Υ_{4s} data above $x_p = 0.5$ which can only arise from continuum events, were fitted with the Peterson fragmentation function[11]:

$$f(x_p) = \frac{a}{x_p}\cdot\left(1 - \frac{1}{x_p} - \frac{\epsilon}{1-x_p}\right)^{-2}, \tag{5}$$

where a is a free normalisation parameter and ϵ is the shape parameter indicating whether the distribution is hard or soft. A value of $\epsilon = (10.8 \pm 1.5) \times 10^{-2}$ is determined, and the integral of the fitted curve gives the continuum D_S^+ production cross section of:

$$\sigma(e^+e^- \rightarrow D_S^+ X)\cdot BR(D_S^+ \rightarrow \phi\pi^+) = (7.5 \pm 0.8 \pm 0.7)\ \mathrm{pb}\,, \tag{6}$$

at an average center of mass energy of 10.5 GeV, in good agreement with our previous measurement.[12] Using the fitted value of ϵ, the continuum contribution in the Υ_{4s} data sample is subtracted, yielding the x_p distribution shown in Fig. 10. This contains a two-body component from decays of the type $B \rightarrow D_S^{(*)}D^{(*)}$ and a broader three-body distribution at lower mean x_p. The former is broadened by effects such as the momentum of the B meson, the additional phase space due to decays $D_S^{*+} \rightarrow D_S^+\gamma$, and the finite detector resolution. Both the two-body and three-body line shapes were calculated by Monte Carlo and fitted to the data: the two curves and the result of the composite fit are shown in Fig. 10. The D_S^+ production cross section is determined from the integral of the fitted curve, divided by the known number of B mesons. The following results are extracted for inclusive D_S production from B decays:

$$BR(B \rightarrow D_S^+ X)\cdot BR(D_S^+ \rightarrow \phi\pi^+) = (2.92 \pm 0.39 \pm 0.31) \times 10^{-3}\,, \tag{7}$$

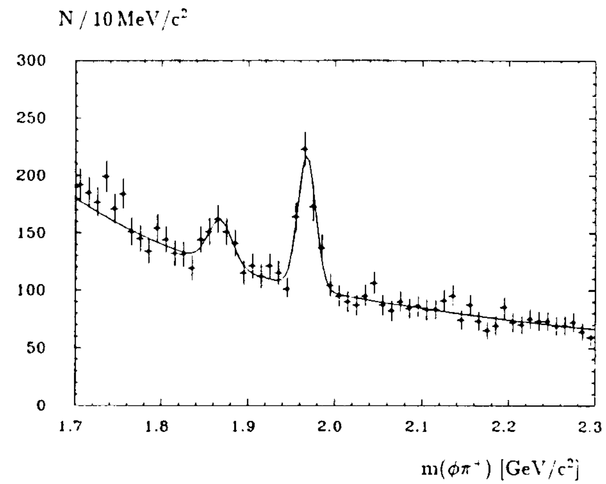

Figure 8: The $\phi\pi^+$ invariant mass distribution from Υ_{4s} data.

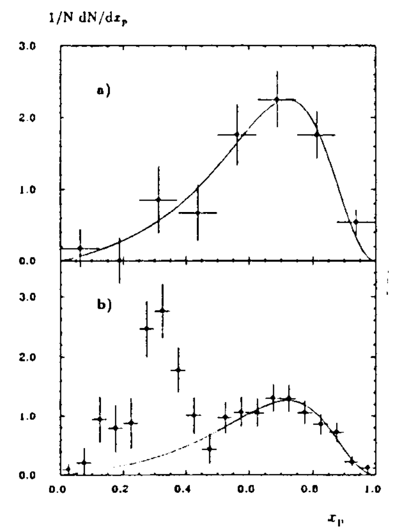

Figure 9: The efficiency corrected x_p distribution for D_S^+ mesons from **(a)** non-resonant $q\bar{q}$ continuum events, and from **(b)** Υ_{4s} data. Solid curve is result of fit with the Peterson fragmentation function.

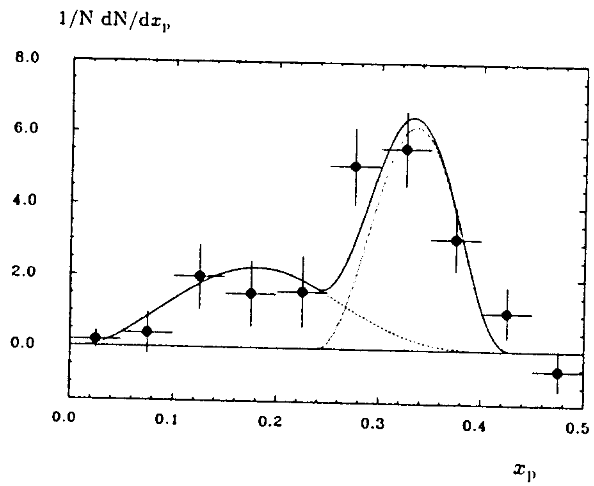

Figure 10: The x_p distribution of D_S^+ mesons from B decays. The solid curve is the composite result of fitting a two-body (dotted curve) and three-body contribution (dashed curve).

$$\text{Two-body component} = (58 \pm 7 \pm 9)\ \% \ . \tag{8}$$

The systematic errors encompass the uncertainties in the continuum subtraction, the efficiency correction, the number of B mesons, and the composition of the two- and three-body spectra. These results are in good agreement with previous results from ARGUS[10] and CLEO.[13,14]

2.3. *Exclusive D_S production*

Encouraged by the strong two-body component seen in the inclusive analysis, the eight exclusive modes of the form $B \to D_S^{(*)}D^{(*)}$ detailed in Table 2 were investigated. Due to small branching ratios and efficiencies, many decay modes of the $D_{(S)}^{(*)}$ mesons were used in the reconstruction.[15] To improve the momentum resolution a mass-constrained fit was applied to all intermediate states having a natural width significantly smaller than the detector resolution (K_S^0, π^0, η', D_S^+, D^0, D^+, D_S^{*+}, D^{*+} and D^{*0}). The D_S^+, D^0, and D^+ candidates are required to have an invariant mass within ± 30, ± 25, and ± 20 MeV/c^2 of their nominal value[16] for two-body, three-body, and four-body decays, respectively. B meson candidates are required to lie within $\pm 3\sigma_E$ of the beam energy, where σ_E is the experimentally determined energy resolution, and then subjected to an energy-constrained fit. Standard topological cuts are applied to suppress continuum events. Details of all the selection criteria are given in a paper under preparation.[15]

The invariant mass distribution of all eight two-body modes is shown in Fig. 11. Fitting this with a constant background and a Gaussian peak to describe the B signal yields:

$$(25.6 \pm 5.6) \text{ events at } M_B = (5279.5 \pm 1.1)\ \text{MeV/c}^2. \tag{9}$$

The shaded histogram in Fig. 11 is the result of applying the same analysis to the continuum data; the background found under the B peak, scaled to the same luminosity as the Υ_{4s} data, is consistent with the background from the fit. Dividing the signal into charged and neutral B decays allows the determination of:

$$M_B^0 - M_B^+ = (-2.7 \pm 2.0 \pm 1.2)\ \text{MeV/c}^2. \tag{10}$$

The systematic error includes the uncertainty on the Υ_{4s} mass, the determination of the beam energy, and the background parameterisation.

The B signal may also be subdivided into the eight exclusive channels. Each mode contains entries at the B mass plus some background, and there is no crosstalk between channels. Fitting the eight distributions with a constant background and a Gaussian peak with width and position fixed from Monte Carlo studies, yields the results in Table 2. Reconstruction efficiencies are determined from detailed Monte Carlo studies and the branching ratios of the charmed mesons are taken from Ref.[16] The D_S^+ branching ratios are only reliably known relative to the BR($D_S^+ \to \phi\pi^+$) so a fixed value of 2.7% was taken from Ref.[16] The uncertainty on this last number is not considered in the results presented in Table

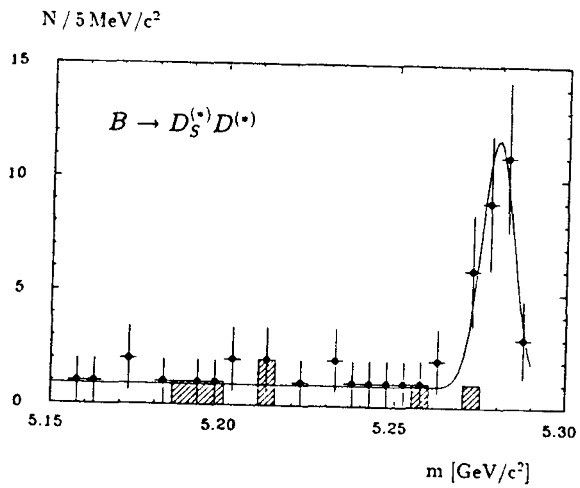

Figure 11: The invariant mass distribution for all eight $B \to D_S^{(*)} D^{(*)}$ decay modes. The solid line shows a fit with a Gaussian peak on a constant background. The hatched histograms shows the unscaled continuum data.

2. The quoted systematic errors include uncertainties on the number of B mesons produced, the D and D^* branching ratios, the procedure used to determine the number of signal events, and the reconstruction efficiency calculations.

Table 2: The branching ratios of decay modes $B \to D_S^{(*)} D^{(*)}$, assuming a fixed value of 2.7% for $BR(D_S^+ \to \phi\pi^+)$. The measurements from the CLEO collaboration[13] are scaled to the same D_S^+ normalization.

B decay mode	Events	Background	Branching ratio	BR from[13]
$B^+ \to D_S^+ \overline{D}^0$	5	0.6 ± 0.3	$(2.4 \pm 1.2 \pm 0.4)\%$	$(2.4 \pm 1.1)\%$
$B^+ \to D_S^{*+} \overline{D}^0$	3	0.7 ± 0.3	$(1.6 \pm 1.2 \pm 0.3)\%$	
$B^+ \to D_S^+ \overline{D}^{*0}$	2	—	$(1.3 \pm 0.9 \pm 0.2)\%$	
$B^+ \to D_S^{*+} \overline{D}^{*0}$	5	0.2 ± 0.1	$(3.1 \pm 1.6 \pm 0.5)\%$	
$B^0 \to D_S^+ D^-$	3	0.6 ± 0.4	$(1.7 \pm 1.3 \pm 0.6)\%$	$(1.1 \pm 0.6)\%$
$B^0 \to D_S^{*+} D^-$	4	0.8 ± 0.4	$(2.7 \pm 1.7 \pm 0.9)\%$	
$B^0 \to D_S^+ D^{*-}$	3	0.4 ± 0.3	$(1.4 \pm 1.0 \pm 0.3)\%$	$(2.0 \pm 1.2)\%$
$B^0 \to D_S^{*+} D^{*-}$	4	0.1 ± 0.1	$(2.6 \pm 1.4 \pm 0.6)\%$	

The branching ratios of Table 2 may best be compared to the predictions of various theoretical models by considering the ratio of ratios. In this manner, the D_S^+ and D branching ratios cancel from the experimental numbers, and ill-determined constants such as V_{cb}, τ_B, and particularly f_{D_S} cancel in the theoretical estimates. The ratios of branching ratios:

$$\frac{B(B^+ \to D_S^{*+}\overline{D}^0)}{B(B^+ \to D_S^+\overline{D}^0)}, \quad \frac{B(B^+ \to D_S^{*+}\overline{D}^{*0})}{B(B^+ \to D_S^+\overline{D}^{*0})}, \quad \frac{B(B^0 \to D_S^{*+}D^-)}{B(B^+ \to D_S^+\overline{D}^0)}, \quad \frac{B(B^0 \to D_S^{*+}D^{*-})}{B(B^0 \to D_S^+D^{*-})},$$

are shown in Fig. 12, along with the corresponding predictions from the models of Bauer-Stech-Wirbel[3] (triangles △), Körner[17] (dots ◯), Hussain-Scadron[18] (squares □), and Mannel-Roberts-Ryzak[19] (diamonds ◇); the latter representing calculations from heavy quark effective theory. Although the errors on the measured ratios of branching ratios are large, the results are in considerably better agreement with the predictions from heavy quark effective theory and the BSW model, than with the approaches of Körner and Hussain-Scadron.

2.4. Determination of the weak decay constant f_{D_S}

Having established that the theoretical branching ratios predicted from the model of BSW and from heavy quark effective theory (HQET) are consistent with the observed results, a value for f_{D_S} may be calculated according to these two schemes. HQET is a relatively new approach for describing the weak decays of heavy mesons[20] in which the mass of the heavy quark is considered to be infinitely large. In this limit, the heavy quark does not feel the recoil of QCD interactions of

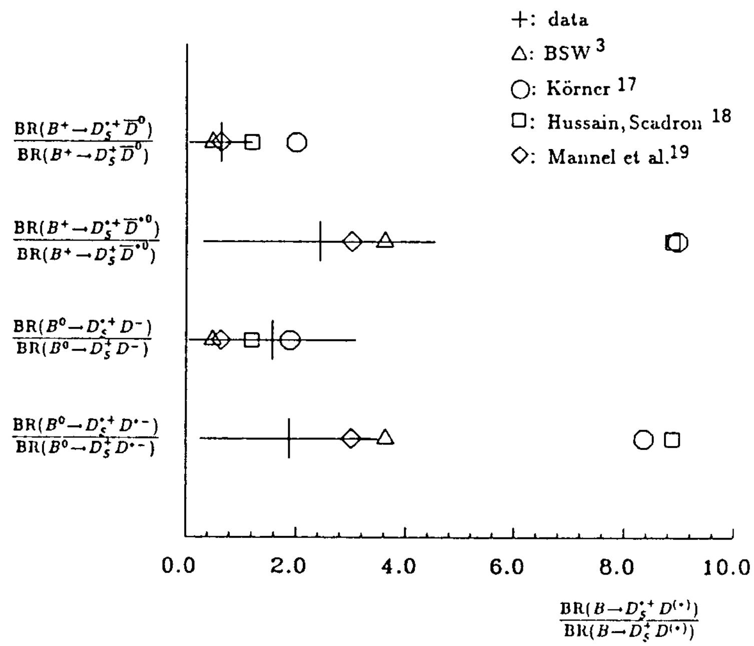

Figure 12: Comparison of the measured ratio of branching ratios (see text) with the corresponding theoretical predictions of different models.

the light anti-quark; the new feature of this theory is that heavy meson decays are governed by a single universal form factor, referred to as the Isgur-Wise function. This may be understood in the perspective of the infinite mass limit where the spin of the heavy quark effectively decouples from that of the light anti-quark spectator, and the form factor then depends only upon the velocity change the light quark must undergo in order to pass from the parent to daughter meson. By definition, this form factor has a magnitude of unity at the zero recoil point (or zero velocity change), but the functional form with which it diverges from unity with increasing velocity transfer, must be specified. Various forms are suggested in the literature[21,19,22]; typically, they contain one slope' parameter that must be determined experimentally.

The idea of HQET may be combined with the factorisation assumption to allow predictions for non-leptonic heavy meson decays. As a test of this assumption, Mannel *et al.*[23] have suggested equal decay widths for $B \rightarrow D_S^{*+}D$ and $B \rightarrow D_S^+D^*$. From the results in Table 2:

$$\Gamma(B \rightarrow D_S^{*+}D)/\Gamma(B \rightarrow D_S^+D^*) = 1.5 \pm 1.0, \tag{11}$$

where the charged and neutral B decays have been averaged. This is compatible with unity, but is not a particularly strong test. A better, but less relevant test, is the prediction of equal decay rates for $B^0 \rightarrow \pi^+D^-$ and $B^0 \rightarrow \pi^+D^{*-}$. Here, the pion momentum spectrum is much harder than that of the D_S^+ meson in the previous case, and the fast pion is more likely to escape without feeling significant strong interaction effects. Dugan and Grinstein[24] suggest that the factorisation assumption is more likely to be valid for such light mesons production. Combining CLEO data from Ref.[25] and recent ARGUS results,[26] the weighted mean values:

$$BR(B^0 \rightarrow \pi^+D^-) = (0.37 \pm 0.06 \pm 0.08)\% \tag{12}$$
$$BR(B^0 \rightarrow \pi^+D^{*-}) = (0.36 \pm 0.07 \pm 0.08)\% \tag{13}$$
$$\text{Average} = (0.37 \pm 0.05 \pm 0.08)\% \tag{14}$$

are in good agreement. The average $BR(B^0 \rightarrow \pi^+D^{(*)-})$ is used below for normalisation purposes.

In view of the cancellation of common systematic uncertainties, it is again advantageous to consider the ratio of branching ratios in extracting a value for f_{D_S}. To calculate the predictions from HQET, the decay rate of a B meson to PV (Pseudoscalar-Vector), PP, and VV final states, as calculated by Rosner,[21] were used. This leads to expressions of the form:

$$\frac{\Gamma(B^0 \rightarrow D_S^+D^-)}{\Gamma(B^0 \rightarrow \pi^+D^-)} = \frac{f_{D_S}^2}{f_\pi^2} \cdot \frac{|V_{cs}|^2}{|V_{ud}|^2} \cdot \frac{|\xi(w_{D_S^+}^2)|^2}{|\xi(w_\pi^2)|^2} \cdot \frac{\lambda^{\frac{1}{2}}(1,\zeta,y_{D_S^+})}{\lambda^{\frac{1}{2}}(1,\zeta,y_\pi)} \cdot \frac{[(1+\sqrt{\zeta})^2 - y_{D_S^+}]^2}{[(1+\sqrt{\zeta})^2 - y_\pi]^2} \tag{15}$$

with $\zeta = (m_D/m_B)^2$, $\lambda(a,b,c) = a^2+b^2+c^2-2ab-2ac-2bc$, $y_P = (m_P/m_B)^2$ and $\xi(w_P^2)$ is the Isgur-Wise function with $w_P^2 = (v-v')^2 = [m_P^2-(m_B-m_D)^2]/m_Bm_D$.

Here, the mass difference $m_{D^*} - m_D$ has been neglected, and f_{D_S} assumed equal to $f_{D_S^*}$ as expected in the heavy quark limit.

Three different analytic forms[21,19,22] were tried for the Isgur-Wise function but resulted in small variations in the final result. As an illustration, Rosner[21] suggests a simple pole hypothesis:

$$\xi(w^2) = \frac{1}{1 - \frac{w^2}{w_0^2}}, \tag{16}$$

where w_0 is the slope' factor, and w is the 4-velocity transfer. At the zero recoil point ($w = 0$) the form factor becomes unity; the slope' factor is determined to be $w_0 = 1.17 \pm 0.20$, obtained by simultaneously fitting the ratios $BR(B \to D\ell\nu)/BR(B^0 \to \pi^+ D^{(*)-})$, $BR(B \to D^*\ell\nu)/BR(B^0 \to \pi^+ D^{(*)-})$, and the polarisation variable $\alpha = 2\Gamma_L/\Gamma_T - 1$ taken from Ref.[27,28]

By comparing the theoretical predictions for the branching ratios $BR(B \to D_S^{(*)} D^{(*)})/BR(B^0 \to \pi^+ D^{(*)-})$ with the measured branching ratios $B \to D_S^{(*)} D^{(*)}$ given in Table 2 and the average value for $BR(B^0 \to \pi^+ D^{(*)-})$ given above, a value $f_{D_S} = (273 \pm 32 \pm 14)$ MeV is found. This is an average of results with different choices of Isgur-Wise function. All such results were in the range 271 - 275 MeV. The systematic uncertainty is dominated by the uncertainty in determining the slope' parameters.

The inclusive measurement of D_S^+ production may also be used to obtain a value for f_{D_S}. Taking the results given in Equations 7 and 8, and using a value for $BR(D_S^+ \to \phi\pi^+) = 2.7\%$, the ratio $BR(B \to D_S^{(*)} D^{(*)})/BR(B^0 \to \pi^+ D^{(*)-})$ gives a value of $f_{D_S} = (255 \pm 45 \pm 13)$ MeV. Since the inclusive and exclusive results are effectively independent, a weighted average of:

$$f_{D_S} = (267 \pm 28)\ \text{MeV} \times [0.027/BR(D_S^+ \to \phi\pi^+)]^{1/2}, \tag{17}$$

is obtained within the framework of HQET. The statistical and systematic errors have been added in quadrature, and the dependence on the branching ratio assumed above for $D_S^+ \to \phi\pi^+$ has been included explicitly.

A value for f_{D_S} may also be extracted from a comparison with the predictions of the BSW[3] model for the ratios of widths $\Gamma(B \to D_S^+ D^{(*)})/\Gamma(B^0 \to \pi^+ D^{(*)-})$ and $\Gamma(B \to D_S^{*+} D^{(*)})/\Gamma(B^0 \to \pi^+ D^{(*)-})$. In this model, both the numerator and denominator of these ratios are expressed in terms of a parameter a_1 which cancels in the ratio, along with other quantities such as V_{cb} and τ_B. The BSW predictions are rescaled in terms of f_{D_S} and $f_{D_S^*}$ according to the values used in Ref.[3] A fit of the four experimentally measured ratios:

$$\frac{\Gamma(B^+ \to D_S^+ \overline{D}^0)}{\Gamma(B^0 \to \pi^+ D^-)}, \quad \frac{\Gamma(B^0 \to D_S^+ D^-)}{\Gamma(B^0 \to \pi^+ D^-)}, \quad \frac{\Gamma(B^+ \to D_S^+ \overline{D}^{*0})}{\Gamma(B^0 \to \pi^+ D^{*-})}, \quad \frac{\Gamma(B^0 \to D_S^+ D^{*-})}{\Gamma(B^0 \to \pi^+ D^{*-})},$$

to the corresponding theoretical predictions, yields $f_{D_S} = (331 \pm 55)$ MeV. Substituting D_S^{*+} for the D_S^+ in these ratios, gives $f_{D_S^*} = (280 \pm 46)$ MeV. If all eight ratios are combined, the result is $f_{D_S} = (298 \pm 36)$ MeV. The results from the analysis of the inclusive data given by Equations 7 and 8 may be used as described above, and a value of $f_{D_S} = (271 \pm 48)$ MeV is extracted. The weighted average of the inclusive and exclusive measurements give a final result of:

$$f_{D_S} = (288 \pm 29)\ \text{MeV} \times [0.027/BR(D_S^+ \to \phi\pi^+)]^{1/2}, \tag{18}$$

based upon the model of Bauer-Stech-Wirbel, in good agreement with the result from HQET. Theoretical estimates[29–45] favour the range between 200 - 300 MeV.

3. A new result[c] for BR($B^- \to D^{*0}\ell^-\overline{\nu}$) and the calculation of V_{cb}

3.1. Introduction

The Cabibbo-Kobayashi-Maskawa element V_{cb} has been extracted from measurements of the semileptonic decay of neutral B mesons to charged D and D^* states.[46,27,47] Additional information may also be obtained from the decay of charged B mesons to the neutral D^* state, but previous studies[48,49] have done so without reconstruction of the D^{*0} meson. Reported here are the preliminary results from the first study of semileptonic B decays where the D^{*0} meson is fully reconstructed. The resulting branching ratio will be used to calculate a value for V_{cb} within the framework of HQET. A paper containing full details of this analysis is under preparation by the ARGUS collaboration. In this work, the theme of presenting results in the context of HQET is continued, preceded by a somewhat cursory description of the analysis.

3.2. Analysis

The data for this analysis consisted of an integrated luminosity of 246 pb^{-1} taken on the Υ_{4s} resonance corresponding to about 209000 ± 10000 $\Upsilon(4S)$ decays. The analysis was performed using an extension of the recoil mass technique successfully used for analysing the semileptonic decays to charged D^* states. In such decays, the neutrino is unobserved but may be inferred if the recoil mass squared against the $D^*\ell^-$ system:

$$M^2_{recoil} = (E_{B^-} - E_{D^*} - E_{l^-})^2 - (\vec{P}_{D^*} + \vec{P}_{l^-})^2 \tag{19}$$

is consistent with zero. The B mesons produced from the decays of the $\Upsilon(4S)$ are known to have the energy of the beam, and to have negligible momentum. For decays to the neutral D^* meson, the success of this technique is somewhat compromised by the large combinatorial background due to soft photons when reconstructing the decay $D^{*0} \to D^0\gamma$. Therefore, events were selected with five or less photons of energy greater than 80 MeV, and π^0 decays were suppressed by eliminating those photon pairs with an invariant mass within $\pm 50\text{MeV}/c^2$ of the π^0 mass. The first cut suppresses the background by a factor of three whilst keeping 60% of the signal; the second cut has a similar efficiency for the signal but reduces the background by a factor of four. The D^0 mesons were reconstructed in their decays to the $K^-\pi^+$, $K^-\pi^+\pi^+\pi^-$ or $K_S{}^0\pi^+\pi^-$ final states.

The $D^0\gamma$ invariant mass distribution so obtained for events containing a well-identified lepton shows a prominent peak at the D^{*0} mass for $|M^2_{recoil}| < 1$ GeV^2/c^4 and a background that is largely described by the distribution obtained from the D^0 sidebands. After sideband subtraction, the remaining background is attributed to continuum events, to uncorrelated $D^0\ell$ combinations, and to correlated $D^0\ell$ accompanied by a random γ. These sources are modeled with detailed Monte Carlo simulations, and subtracted. By analogy, the resulting D^{0*} signal contains some background contributions from the continuum, and from uncorrelated $D^{*0}\ell$ pairs. Again, these are estimated from Monte Carlo calculations. The possibility of an additional background from the cascade decays of the D^{**} state must also be considered. In principle this may be estimated from the data since these events will have a different recoil mass squared distribution than the direct decays to the D^{*0}. The signal is therefore fitted in separate bins of recoil mass squared and the resulting distribution, shown in Fig. 13, is fitted with the sum of two Gaussians corresponding to the contributions from the signal and cascade decays.

The fit yields a signal amplitude of 224±44 events in the region $|M^2_{recoil}| < 1.0$ GeV^2/c^4. The D^{**} contribution is found to be -14 ± 61 events over the whole recoil mass interval, about half of which is applicable to the signal region. Therefore, a contribution of 0 ± 31 events is assumed, giving a signal of 224 ± 54 events. Correcting this result for all the selection efficiencies, gives a branching ratio:

$$BR(B^- \to D^{*0}e^-\bar{\nu}) = BR(B^- \to D^{*0}\mu^-\bar{\nu}) = 5.8 \pm 1.4 \pm 1.3\% \,, \qquad (20)$$

where the first error is statistical and the second is systematic. Although these errors are relatively large, this is the first analysis of this decay mode to reconstruct the D^{*0} meson.

3.3. *Calculation of V_{cb} from HQET*

To measure V_{cb} the momentum distribution of the D^{*0} mesons is used to determine the product $V_{cb} \cdot \xi(y)$, where ξ is the universal Isgur-Wise form factor. Here, the form factor is expressed as a function of $y = E_{D^*}/m_{D^*}$ and, following Neubert,[50] $\xi(1)$ is determined by extrapolation from the full momentum interval. Figure 14 shows $|V_{cb}|\,\xi(y)$ extracted from the data using the following formula:

$$|V_{cb}|\,\xi(y) = \frac{1}{\sqrt{y^2-1}}\frac{d\Gamma}{dy}\frac{48\pi^3}{G_F{}^2 m_{D^*}{}^3(m_B - m_{D^*})^2(1+\beta_{A_1}\alpha_s(m)/\pi)^2(F_T(y)+F_L(y))} \qquad (21)$$

where the definitions of $F_T(y)$, $F_L(y)$, and β_{A_1} can be found in Ref.[50]

The shape of the form factor is open to interpretation, and in this analysis a linear parameterization of the form $\xi(y) = 1 - \rho^2(1-y)$ was used. Thus, the data in Fig. 14 were fitted with a straight line giving a slope $\rho = 1.07 \pm 0.17$

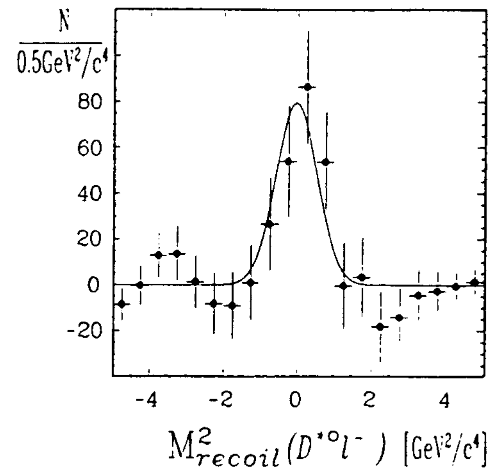

Figure 13: $M^2_{recoil}(D^{*0}l^-)$ distribution after subtraction of all backgrounds. The line represents the fit result for the decay $B^- \to D^{*0}\ell^-\bar{\nu}$.

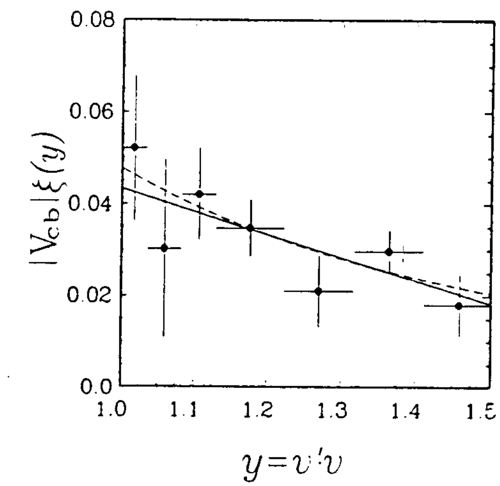

Figure 14: The distribution of $|V_{cb}|\,\xi(y)$ calculated from the momentum distribution of the D^{*0} mesons. The data points are fitted with a linear (solid curve) and a simple pole (dashed curve) parameterisation of the Isgur-Wise function.

and an intercept at zero recoil ($y = 1$) of $|V_{cb}| = 0.045 \pm 0.007$ using $\tau_B = (1.24 \pm 0.09 \pm 0.12) \times 10^{-12}$ seconds.[51] Similar results are obtained for $|V_{cb}|$ under different parameterisations for the Isgur-Wise function. For example, a fit with a single pole parameterisation[50] gives $\rho = 1.30 \pm 0.028$ and $|V_{cb}| = 0.047 \pm 0.009$, and is shown by the dashed line in Fig. 14. Adding, in quadrature, the effects of the systematic errors on the branching ratio to the result of the linear fit, gives:

$$|V_{cb}| = 0.045 \pm 0.009 \tag{22}$$

in good agreement with previous results.[16]

* The current members of the ARGUS collaboration are: H. Albrecht, H. Ehrlichmann, T. Hamacher, A. Krüger, A. Nau, A. Nippe, S. Nowak, M. Reidenbach, M. Schäfer, H. Schröder, H. D. Schulz, M. Walter, R. Wurth, (DESY, Germany), R. D.Appuhn, C. Hast, G. Herrera, H. Kolanoski, A. Lange, A. Lindner, R. Mankel, M. Schieber, T. Siegmund, B. Spaan, H. Thurn, D. Töpfer, A. Walther, D. Wegener (Universität Dortmund, Germany), M. Paulini, K. Reim, H. Wegener, (Universität Erlangen-Nürnberg, Germany), R. Mundt, T. Oest, W. Schmidt-Parzefall, (Universität Hamburg, Germany), W. Funk, J. Stiewe, S. Werner, (Universität Heidelberg, Germany), K. Ehret, A. Hölscher, W. Hofmann, S. Khan, K. T. Knöpfle, J. Spengler, (MPI, Heidelberg, Germany), D. I. Britton, C. E. K. Charlesworth, K. W. Edwards, H. Kapitza, P. Krieger, D. B. MacFarlane, P. M. Patel, J. D. Prentice, S. C. Seidel, K. Tzamariudaki, R. G. Van de Water, T.-S. Yoon, (IPP, Canada), D. Reßing, M. Schmidtler, M. Schneider, K. R. Schubert, K. Strahl, R. Waldi, S. Weseler, (Universität Karlsruhe, Germany), G. Kernel, P. Križan, E. Križnič, T. Podobnik, T. Živko, (Univerza v Ljubljani, Slovenia), H. I. Cronström, L. Jönsson, (University of Lund, Sweden), V. Balagura, I. Belyaev, M. Danilov, A. Droutskoy, B. Fominykh, A. Golutvin, I. Gorelov, G. Kostina, V. Lubimov, P. Murat, P. Pakhlov, F. Ratnikov, A. Rostovtsev, A. Semenov, S. Semenov, V. Soloshenko, I. Tichomirov, Yu. Zaitsev, (ITEP, Moscow, USSR).

[a] Thesis work of T. Oest.

[b] Thesis work of M. Paulini.

[c] Thesis work of P. Pakhlov.

References

1. H. Albrecht et al.,(ARGUS), Phys. Lett. **B234** (1990) 409.
   R. Fulton et al.,(CLEO), Phys.Rev.Lett. **64** (1990) 16.
2. H. Albrecht et al.,(ARGUS), Phys. Lett. **B255** (1990) 297.
3. M.Wirbel, B.Stech and M.Bauer, Z.Phys. **C29** (1985) 637.
   Z.Phys. **C34** (1987) 103; Z.Phys. **C42** (1989) 671.
4. J. G. Korner and G.A. Schuler, Z.Phys. **C38** (1988) 511.
5. N.Isgur, D.Scora, B.Grinstein and M.B.Wise, Phys. Rev. **D39** (1989) 799.
6. G. Kramer and W.F. Palmer, Phys. Rev. **D42** (1990) 85.
7. G. Kramer et al., DESY preprint 90-168 (1990).
8. G. Altarelli et al., Nucl.Phys. **B208** (1982) 365.
9. H. Albrecht et al.,(ARGUS), Nucl.Instr.Methods **A275** (1989) 1.

10. H. Albrecht et al.,(ARGUS), Phys.Lett. **B187** (1987) 425.

11. C. Peterson et al., Phys.Rev. **D27** (1983) 105.

12. H. Albrecht et al.,(ARGUS), Phys.Lett. **B207** (1988) 349.

13. D. Bortoletto et al.,(CLEO), Phys.Rev.Lett. **64** (1990) 2117.

14. P. Haas et al.,(CLEO), Phys.Rev.Lett. **56** (1986) 2781.

15. H. Albrecht et al.,(ARGUS), Paper entitled Production of D_S^+ Mesons in B Decays and the Determination of f_{D_S}' currently in preparation.

16. Particle Data Group, Phys.Lett. **B239** (1990) 1.

17. J. G. Körner, in Proceedings of the International Symposium on Production and Decay of Heavy Hadrons, Heidelberg, Germany, edited by K. R. Schubert and R. Waldi, 1986.

18. F. Hussain, M. D. Scadron, Phys.Rev. **D30** (1984) 1492.

19. T. Mannel, W. Roberts, Z. Ryzak, Harvard preprint, HUTP-91/A069 (1991), submitted to Phys.Lett. **B**.

20. M. Voloshin, M. Shifman, Sov.J.Nucl.Phys. **45** (1987) 292 and Sov.J.Nucl.Phys. **47** (1988) 511;
E. Eichten, B. Hill, Phys.Lett. **B234** (1990) 511;
H. Politzer, M. Wise, Phys.Lett. **B206** (1988) 681 and Phys.Lett. **B208** (1988) 504;
N. Isgur, M. Wise, Phys.Lett. **B232** (1989) 113 and Phys.Lett. **B237** (1990) 527;
B. Grinstein, Nucl.Phys. **B339** (1990) 253;
H. Georgi, Phys.Lett. **B240** (1990) 447;
J. D. Bjorken, SLAC preprint, SLAC-PUP-5278 (1990);
A. Falk, H. Georgi, B. Grinstein, M. Wise, Nucl.Phys. **B343** (1990) 1;
A. Falk, B. Grinstein, Phys.Lett. **B247** (1990) 406.

21. J. L. Rosner, Phys.Rev. **D42** (1990) 3732.

22. M. Neubert, V. Rieckert, Heidelberg preprint, HD-THEP-91-6 (1991), submitted to Nucl.Phys. **B**.

23. T. Mannel, W. Roberts, Z. Ryzak, Harvard preprint, HUTP-91/A011 (1991).

24. M. J. Dugan, B. Grinstein, Phys.Lett. **B255** (1991) 583.

25. D. Cassel (CLEO), Proceedings of Physics in Collision 10, Duke University, Durham, Ed. A. Goshaw, L. Montanet, World Scientific, Singapore, 1990.

26. H. Albrecht et al.,(ARGUS), Z.Phys. **C48** (1990) 543.

27. H. Albrecht et al.,(ARGUS), Phys.Lett. **B219** (1989) 121.

28. D. Bortoletto et al.,(CLEO), Phys.Rev.Lett. **63** (1989) 1667.

29. H. Krasemann, Phys.Lett. **B96** (1980) 397.

30. S. Godfrey, N. Isgur, Phys.Rev. **D32** (1985) 189.

31. M. Suzuki, Phys.Lett. **B162** (1985) 392.

32. S. N. Sinha, Phys.Lett. **B178** (1986) 110.

33. P. Cea et al., Phys.Lett. **B206** (1988) 691.

34. D. Silverman, H. Yao, Phys.Rev. **D38** (1988) 214.

35. S. Capstick, S. Godfrey, Phys.Rev. **D41** (1990) 2856.

36. E. Golowich, Phys.Lett. **B91** (1980) 271.

37. V.S. Mathur, T. Yamawaki, Phys.Lett. **B107** (1981) 127; Phys.Rev. **D29** (1984) 2057.

38. D.A. Dominquez, N. Paver, Phys.Lett. **B197** (1987) 427; Phys.Lett. **B199** (1987) 596(E).

39. S. Narison, Phys.Lett. **B198** (1987) 104.

40. M.A. Shifman, Ups.Fiz.Nauk **151** (1987) 193; Sov.Phys.Ups. **30** (1987) 91.

41. M.B. Gavela et al., Phys.Lett. **B206** (1988) 113.

42. D.A. DeGrand, R.D. Loft, Phys.Rev. **D38** (1988) 954.

43. C. Bernard et al., Phys.Rev. **D38** (1988) 3540.

44. R.M. Woloshyn et al., Phys.Rev. **D39** (1989) 978.

45. C. Alexandrou et al., Phys.Lett. **B256** (1991) 60.

46. H.Albrecht et al., (ARGUS), Phys.Lett. **B197** (1987) 452.

47. H.Albrecht et al., (ARGUS), Phys.Lett. **B229** (1989) 175.

48. R.Fulton et al., (CLEO), Phys.Rev. **D43** (1991) 651.
Branching ratios have been adjusted to reflect current best values for D^0 decays.[16]

49. D.Antreasyan et al., (Crystal Ball), Z.Phys. **C48** (1990) 553.

50. M.Neubert,Heidelberg preprint HD-THEP-91-13 (1991).

51. D.Decamp et al., (ALEPH), CERN preprint, PRE/90-116.